Polyvalent Diazonium Polymers Provide Efficient Protection of Oncolytic Adenovirus Enadenotucirev from Neutralising Antibodies while Maintaining Biological Activity *In Vitro* and *In Vivo*

Nora Francini[a,‡], Daniel Cochrane[b], Sam Illingworth[b], Laura Purdie[a], Giuseppe Mantovani[a], Kerry Fisher[b,c], Leonard W. Seymour[c]*, Sebastian G. Spain[d]* and Cameron Alexander[a]*

a. School of Pharmacy, University of Nottingham, NG7 2RD, UK. E-mail: cameron.alexander@nottingham.ac.uk; Tel: +44 (0)115 846 7678.

b. PsiOxus Therapeutics Limited, 4-10, The Quadrant, Abingdon Science Park, Abingdon, Oxfordshire, OX14 3YS, UK.

c. Department of Oncology, Old Road Campus Research Building, Roosevelt Drive, Oxford, OX3 7DQ, UK. Email: len.seymour@oncology.ox.ac.uk.

d. Department of Chemistry, University of Sheffield, Sheffield, S3 7HF. E-mail s.g.spain@sheffield.ac.uk; Tel: +44 (0)114 222 9362; Twitter: @sebspain.

‡ Present address. IIT Central Research Laboratory, Istituto Italiano di Tecnologia, 16163 Genova, Italy.

Abstract.

Oncolytic viruses offer many advantages for cancer therapy when administered directly to confined solid tumors. However, the systemic delivery of these viruses is problematic due to host immune response, undesired interactions with blood components and inherent targeting to the liver. Efficacy of systemically administered viruses has been improved by masking viral surface proteins with polymeric materials resulting in modulation of viral pharmacokinetic profile and accumulation in tumors *in vivo*. Here we describe a new class of polyvalent reactive polymer based upon poly(*N*-(2-hydroxypropyl)methacrylamide) (polyHPMA) with diazonium reactive groups and their application in the modification of the chimeric group B oncolytic virus enadenotucirev (EnAd). A series of six copolymers with different chain lengths and density of reactive groups was synthesised and used to coat EnAd. Polymer coating was found to be extremely efficient with concentrations as low as 1 mg/mL resulting in complete (>99%) ablation of neutralising antibody binding. Coating efficiency was found to be dependent on both chain length and reactive group density. Coated viruses were found to have reduced transfection activity both *in vitro* and *in vivo,* with greater protection against neutralising antibodies resulting in lower transgene production. However, in the presence of neutralising antibodies some *in vivo* transgene expression was maintained for coated virus compared to the uncoated control. The decrease in transgene expression was found not to be solely due to lower cellular uptake but due to reduced unpackaging of the virus within the cells and reduced replication indicating that polymer coating does not cause permanent inactivation of the virus. These data suggest that virus activity may be modulated by appropriate design of coating polymers while retaining protection against neutralising antibodies.

Introduction

Virus-based therapies for cancer were first proposed over 100 years ago but the first clinical trials involving administration of attenuated viruses were of mixed success.(*1*),(*2*) As our understanding of virology has improved conditionally-replicating viruses that can act as anticancer agents (oncolytic viruses)(*3*),(*4*),(*5*) have been developed. These have led to the first product, Oncorine, an engineered oncolytic adenovirus approved for the treatment of head and neck cancer, being released in China in 2005.(*6*),(*7*) More recently, Imlygic, an oncolytic herpes virus, has been approved in US and EU, for the treatment of unresectable melanoma lesions.(*8*)

The widespread use of oncolytic viruses for disseminated cancers via systemic (i.e. intravenous) administration remains limited by virus immunogenicity, and the pharmacokinetic and biodistribution profiles of injected nanoparticles.(*9-11*) Accordingly, there have been efforts to target viruses to cancer sites, in a manner analogous to those adopted for targeting synthetic nanoparticles.(*12-15*) The conjugation of synthetic polymers to provide 'stealth' coatings for oncolytic viruses is one means by which extended circulation and tumour targeting might be achieved. A number of papers have reported successful conjugation of polymers to synthetic viruses,(*16-18*) with concomitant changes in viral biodistribution and targeting.(*19-22*) PEGylation of adenovirus (Ad) was reported in the pioneering work of O'Riordan *et al.*(*23*) and Croyle *et al.*(*24*) Adenovirus (Ad) vectors were modified with PEG_{5000} and were shown to retain infectivity and to transduce cells *in vitro* and *in vivo* in the presence of neutralizing antibodies. Although this was the first example of successfully chemically modified Ad, the study was limited to intranasal delivery and a limited degree of PEGylation, due to aggregation and precipitation of more highly functionalized viruses. Other polymers have been used to coat viruses,(*25*) of which the most widely used has been poly(*N*-(2-hydroxypropyl)methacrylamide) (polyHPMA), covalently bound to the amine groups on the

viral surface. polyHPMA with modified side-chains is a polyvalent polymer, thus the coating of viral surfaces is more dense with this polymer and lower concentrations are required when compared to PEG.(*26*) polyHPMA for Ad shielding was first developed as a random copolymer with pendant amino-reactive 4-nitrophenolate ester linked to polyHPMA by a gly-gly dipeptide spacer.(*27*),(*28*) In these studies, coating resulted in ablation of Coxsackie-Adenovirus Receptor (CAR) binding and conferred partial resistance to neutralizing antibodies. Extended plasma circulation was observed for polyHPMA coated virus with higher doses achieving longer half-life, to the extent that a 10-fold higher concentration of polyHPMA-Ad was found in plasma 30 minutes after injection compared to naked Ad virus. A marked decrease in virus hepatotoxicity of Ad upon coating with HPMA polymers, was reported, and additional *in vivo* studies showed accumulation of the conjugate in tumor masses after injection and a 40-fold increase in transgene expression compared to unmodified Ad.(*29*) Coating with this copolymer prevented cellular uptake but transfection was restored and boosted when retargeting agents such as fibroblast growth factor 2 (FGF2),(*30*) epidermal growth factor (EGF)(*31*) or cell-penetrating peptides(*32*) were covalently attached. The ability to retarget Ad was evaluated *in vitro* and *in vivo* where a highly efficient and ligand-dependent transduction was observed. However, while a degree of protection against neutralizing antibodies(*27*),(*33*) and improved pharmacokinetic and biodistribution profiles compared to unmodified-Ad viruses(*34*) have been obtained, complete neutralization of antibody responses by polymer conjugation has still to be accomplished.

Accordingly, we set out to develop new methods for polymer conjugation to viruses in order to increase the reaction at the virus surface and therefore enhance the protection against neutralising antibodies. Conjugation strategies of polymers to surface viral proteins usually involves reaction with the ε-amino groups of lysine residues. The natural abundance of this amino acid on viral surfaces, which for adenovirus has been reported to number over 1800

copies(*35*) make it an important target. However, though the use of this strategy has shown relatively high coverage of surface proteins(*22-24, 27*) as demonstrated by 50 to 80% lower anti-adenovirus antibody recognition compared to naked virus, it has failed to produce the complete viral antigen masking that is required for the application of viral therapeutics *in vivo*. Herein, we report the synthesis of new polymers with broadened reactivity towards a variety of amino acid residues – potentially overcoming the limitation suffered from specific lysine targeting – and the effects of these polymers on viral vectors *in vitro* and *in vivo*.

Results and Discussion

Synthesis of functional poly(*N*-(2-hydroxypropyl)methacrylamide) derivatives

The intial aims were to i) utilise a reactive functional group with broad reactivity and ii) determine the effects of polymer chain length and reactive group density on the efficiency of polymer coating of an adenoviral vector. EnAd (and reporter transgene derivatives(*36*)) was selected for these studies since intravenous delivery to tumours has been demonstrated with this virus,(*37*) so modifications that improved delivery efficiency or avoidance of neutralizing antibodies could have direct therapeutic relevance. The synthetic approach is outlined in Fig. 1. PolyHPMA was synthesised via reversible addition-fragmentation chain transfer (RAFT) polymerization which allowed polymers of well-defined chain length to be synthesised. In previous work, we demonstrated that the pendant secondary hydroxyl group of polyHPMA could be modified via a one-step procedure with allyl isocyanate to yield allyl-functional reactive polyHPMA derivatives.(*38*) Here, aniline groups were introduced at different densities along the polyHPMA backbone by reaction with Boc-protected aminobenzoic acid followed by deprotection of amino groups. The aniline groups could then be activated to form highly reactive diazonium groups that would react with the virus surface. The low selectivity of

diazonium coupling for specific amino acids at neutral pH was identified as a possible advantage that may allow reaction with a wider range of sites on the virus surface leading to improved coverage.

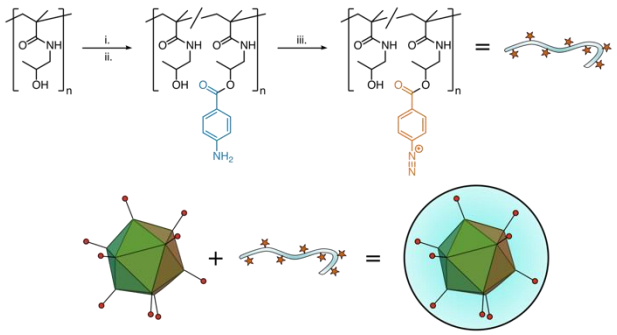

Figure 1. Synthetic outline for the production of polymer-coated viruses from polyvalent diazonium salts. Reagents: i. *N*-Boc-4-aminobenzoic acid, EDC, DMAP, DMSO; ii. TBAF; iii. CF_3CO_2H, $NaNO_2$, sulfamic acid.

A series of polyHPMA homopolymers was synthesized as described by Scales *et al*.(*39*) The chain transfer agent (CTA) to initiator ratios ([CTA]:[I]) were kept constant at 3:1, while the HPMA monomer:CTA ratios were varied, (100, 250, 350) to obtain polymers with different chain lengths, **P1**–**P3** (Table 1). The end-groups introduced during RAFT polymerization are a potential source of toxicity.(*40*) Consequently they were removed as described by Perrier et al.(*41*) End-group removal was confirmed by UV-Vis spectrophotometry (Figure S1) and Ellman's assay (Table 1), performed before and after treatment.

Table 1. Poly[*N*-(2-hydroxypropyl)methacrylamide] precursors

Sample	DP_n	M_n, *(kDa)*		Đ[b]	%Thiol[c]
		Theor[a]	SEC[b]		
P1	85	12.2	17.0	1.11	—[d]
P2	165	23.7	30.3	1.14	—[d]
P3	240	34.3	45.9	1.11	0.32

[a] Calculated considering the initial [HPMA]/[CTA] ratio and final conversion; [b] Determined by SEC using DMF + 0.1 % LiBr as the mobile phase calibrated with PMMA standards; [c] Residual thiol after CTA removal using AIBN, as determined by Ellman's assay.[d] Below detection limit.

Pendent aniline groups were attached to the polymer backbone via the coupling reaction of *N*-*t*-butoxycarbonyl-4-aminobenzoic acid with the hydroxyl groups of polyHPMA, using EDC

and DMAP, as reported by Jones et al. for the esterification of hydroxy-terminated PEG.(*42*) The reactivities of diazonium salts have been demonstrated to increase when electron-withdrawing groups are introduced in the *para* position of the aromatic ring, therefore, in analogy to data reported by Jones *et al*.,(*42*) 4-aminobenzoic acid (PABA) was selected here to generate a polymeric diazonium precursor (hereafter referred to as polyvalent diazonium). Standard Boc protection of commercially available 4-aminobenzoic acid was carried out to afford the pure product (PABA-Boc, Figure S2). The Steglich esterification of alcohols mediated by carbodiimides is often carried out in the presence of catalytic amounts of DMAP. However, under these conditions, a large excess of DMAP was found to be needed to promote the reaction. The optimized reaction was monitored by ^{1}H NMR spectroscopy for 48 h. when no further conversion of the alcohol into the corresponding benzoic esters was observed. Coupling of PABA-Boc to the PHPMA precursors was tailored to target degrees of functionalization of 0.15 and 0.30 aniline groups per initial OH group. Higher modifications (0.5) resulted in unusable water-insoluble polymers after deprotection while lower modifications (0.10 or single terminal modification) failed to undergo later diazo coupling when bioconjugation was tested with a model protein (data not shown).

Benzoic acid content in the final products was quantified by ^{1}H NMR spectroscopy by comparing the reference integral values of the propyl C*H*O, whose summed value was assigned to 1 proton, and the integrals of the aromatic protons or the NH proton of the Boc protecting group. To validate the results, alternatively, the signal of the Boc NH was used as a reference and compared to values of polyHPMA signals. Polyvalent diazonium precursors were treated with 8 equivalents of tetrabutylammonium fluoride (Bu_4NF) to aniline groups at 80 °C for 16 h in DMSO in order to remove the protecting group. The reaction yielded the desired aniline-modified polymers with only limited hydrolysis of the ester groups. ^{1}H NMR spectroscopy was used to assess the removal of Boc groups and to determine the final aniline content (Figure 2).

Six polyvalent diazonium precursors were generated using this method with 3 different chain lengths and 2 degrees of functionalization (Table 2).

As these polymers bear multiple activated aromatic rings in close proximity to each other, there is significant potential inter- and intra-molecular side reactions that would effectively limit the

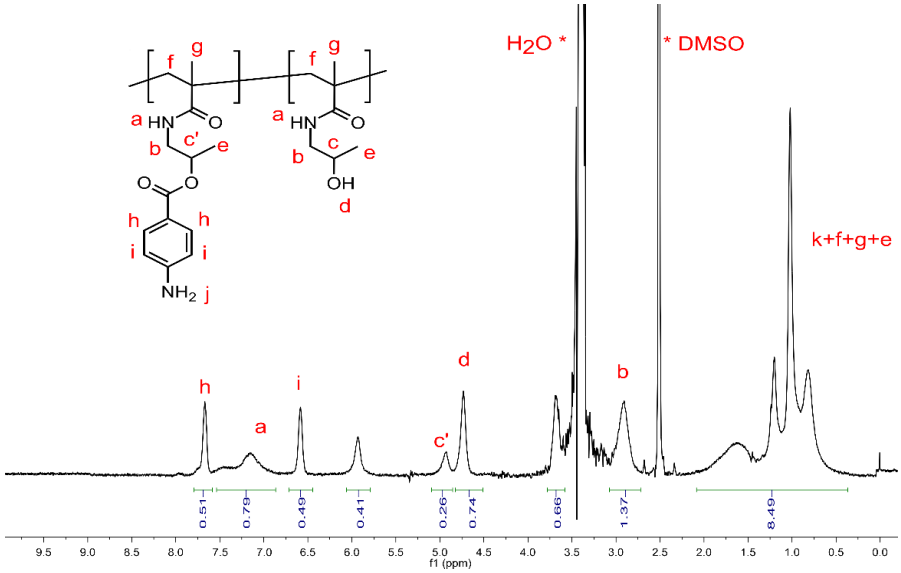

number of diazo groups available for coupling to the desired target. Consequently, the ability of polydiazonium polymers to react completely to give the required diazo-adducts was tested

Figure 2. ^{1}H NMR spectrum of deprotected **P9** in DMSO-d6. All polymers in the **P4**–**P9** library gave analogous spectra, where only the relative intensity of the PABA-Boc and HPMA repeating units was found to change.

and monitored by ^{1}H NMR spectroscopy. The shift in aromatic signals of the aromatic groups in the ^{1}H NMR spectra were used to monitor conversion at each step of the synthesis (Figure 3).

Table 2. Degree of functionalization of PHPMA precursors after post-polymerization modification with *N*-Boc-4-aminobenzoic acid and subsequent deprotection.

	Composition	$PABA_{targ}$ (%)[a]	$PABA_{calc}$ (%)[b,c]	$PABA_{dep}$ (%)[c,d]
P4	$HPMA_{85}$-*r*-$PABA_{9}$	15	11	10
P5	$HPMA_{85}$-*r*-$PABA_{20}$	30	24	24
P6	$HPMA_{165}$-*r*-$PABA_{18}$	15	12	11
P7	$HPMA_{165}$-*r*-$PABA_{40}$	30	25	25
P8	$HPMA_{240}$-*r*-$PABA_{22}$	15	12	9
P9	$HPMA_{240}$-*r*-$PABA_{58}$	30	26	24

[a] targeted based on the initial HPMA:PABA ratio; [b] after esterification; [c] calculated using ^{1}H NMR spectroscopy in DMSO-d_6; [d] after deprotection with Bu_4NF.

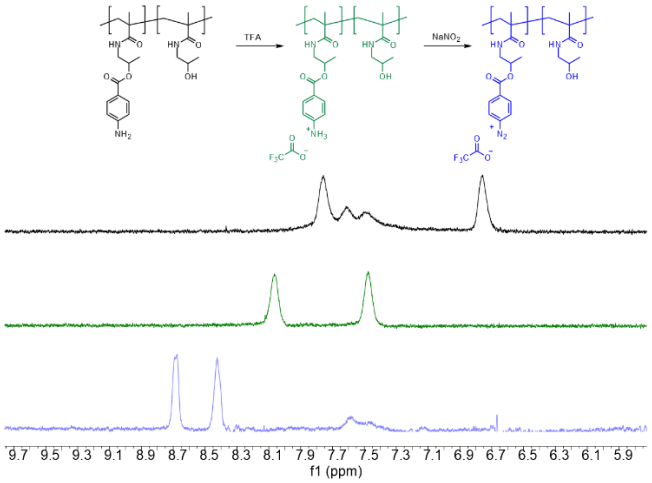

Figure 3. Stacked aromatic region of ^{1}H NMR spectra of the various stages of diazonium salt formation: aniline precursor (black, top), protonated aniline (green, middle) and diazonium salt (blue, bottom).

Diazonium salts of **P7** were generated by sequential addition of TFA and $NaNO_2$ to an aqueous solution of the polymer at 0 °C to form the nitrous acid required to convert the PABA repeating units into their corresponding diazonium salts *in situ*. Excess nitrous acid was quenched and with sulfamic acid and the pH adjusted to 7.4 for subsequent protein conjugation. Control of the reaction temperature was essential for successful diazonium formation with small increases due to addition of mild/warm solutions resulting in decomposition.

Polyvalent diazonium polymers provide efficient shielding of EnAd against neutralizing antibodies *in vitro*

Efficient shielding of the viral surface is essential to prevent recognition, and subsequent destruction, by the immune system. Consequently, the ability of polyvalent diazonium polymers to effectively shield EnAd from neutralizing antibodies was evaluated. The series of

polymers synthesized allowed three variables in the coating to be assessed: the density of diazonium moieties on the polymer chain (i.e. 10 and 24 mol %); the copolymer degree of polymerization (i.e. 85, 165 and 240 units) and the concentration of the copolymers in the conjugation reaction (0.5 to 5.0 mg/mL). The EnAd concentration was kept constant throughout.

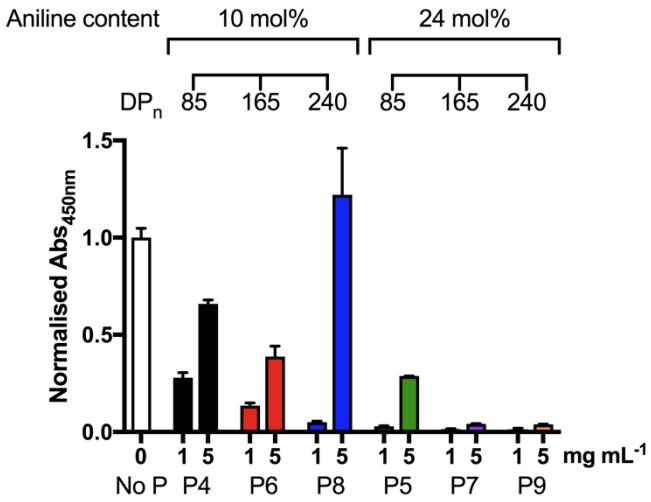

Figure 4. EnAd shielding from neutralizing antibodies as a means of determining polymer coating efficiency determined via ELISA. Values are normalized to uncoated virus control.

The bioconjugation of polyvalent diazonium polymers to was first tested using BSA as a model protein (Figure S3). For virus bionconjugation, stock solutions of **P4** to **P9** were activated *in situ* and added to the required virus aliquot on ice. Three independent experiments were performed with triplicate samples of each formulation. The efficiency of coating was estimated using an enzyme-linked immunosorbent assay (ELISA) with antibodies for EnAd. Briefly, anti-Ad antibody (polyclonal rabbit) was immobilised on an ELISA plate to act as a capture antibody then solutions of unmodified and polymer-coated EnAd were added. The amount of captured EnAd was determined by addition of anti-Ad antibody (polyclonal mouse) which was detected using an anti-mouse HRP secondary antibody with 3,3',5,5'-tetramethylbenzidine (TMB) as the substrate. The absorbance relative to unmodified EnAd was then used to estimate

shielding efficiency i.e. a lower absorbance indicates less bound EnAd and therefore more efficient coating . Represntative results for the six polymers are shown in Figure 4.

At a polymer concentration of 5 mg/mL, the formation of a yellow precipitate was observed after coating with the polymers carrying the higher diazonium content (~24 mol%) indicating the formation of undesired cross-linked viral particle aggregates. Conversely, the lower diazonium content polymers (~10 mol%) did not produce sufficient viral shielding, with the intermediate chain length (DP = 165) achieving around 60% protection against neutralising antibodies. Unexpectedly, the absorbance of **EnAd-P8** exceeded the value observed for the uncoated viral control which would indicate an increase in antibody binding. This was attributed to the combined effect of inefficient polymer coating, resulting in significant antibody binding, and the absorbance in the same spectral region as the ELISA substrate (450 nm)[43] of any azobenzene linkages present.

As cross-linked aggregates are potentially too large for systemic delivery, polymer concentrations of 1, 0.75 and 0.5 mg/mL were investigated to reduce the possibility of polymer-mediated crosslinking. The optimal coating concentration was found to be 1 mg/mL at which all polymers provided viral shielding without the formation of precipitates or aggregates, as confirmed by dynamic light scattering (DLS, table 3). Lower polymer concentrations resulted in insufficient and highly variable coating efficiency (data not shown). At 1 mg/mL polymer concentration, the coating efficiency of polymers with low aniline content (10 mol%) increased with polymer M_n, indicating that larger polymers do improve shielding, with viral shielding as high as 90%. High coating efficiency – defined as reaching 99% viral shielding from neutralising antibodies – was obtained with polymers with higher aniline content (24 mol%), independent of the degree of polymerization. It is worth noting, that **EnAd-P4**, **EnAd-P6** and **EnAd-P8** (10 mol % diazonium) showed higher variability in the outcome of the coating within

the triplicate experiments, indicating that a higher diazonium content might be required to increase the reproducibility of the coating.

Table 3. Hydrodynamic diameter of polymer-coated virus at 1mg/mL coating concentration.

	diameter (nm)	PDI
EnAd	99 ± 1.7	0.1 ± 0.0
EnAd-P4	100 ± 1.6	0.1 ± 0.0
EnAd-P5	107 ± 1.5	0.1 ± 0.0
EnAd-P6	110 ± 2.9	0.1 ± 0.0
EnAd-P7	133 ± 1.0	0.2 ± 0.0
EnAd-P8	108 ± 7.2	0.1 ± 0.1
EnAd-P9	153 ± 6.9	0.1 ± 0.0

Dynamic light scattering (DLS) analysis of the polymer-coated virus formulations, indicated an increase in the hydrodynamic diameter upon coating that can be related to the polymer chain length and capsid shielding (table 3). **EnAd-P4**, **EnAd-P6** and **EnAd-P8**, which displayed less antibody shielding by ELISA, did not present significant increases in their sizes compared to unmodified virus. **EnAd-P5**, **EnAd-P7** and **EnAd-P9**, displayed an increase in the diameter that was polymer chain length-dependent, in agreement with the polymer shielding observed by ELISA.

Previous reports of polymer-coating viruses with polyHPMA have relied upon active esters (e.g. nitrophenolates) as the reactive moiety with surface amines (lysines) as the target on the viral capsid. Typically, active ester chemistries have required high polymer concentrations (20 mg/mL) to achieve antibody shielding with 50–70% reduction in binding as estimated by ELISA.(*33*),(*34*),(*31*) Consequently, achieving high levels of shielding (up to 99%) at low polymer concentrations (1 mg/mL) demonstrates the benefit of using diazonium groups as the reactive species.

In vitro and *in vivo* luciferase expression of polymer-coated EnAd

Although polymer coating can prevent antibody binding, it can also affect the biological activity of the virus by preventing interactions with cell surfaces (and thus viral uptake) and

viral unpacking (and thus gene expression and virus replication). To determine whether EnAd activity was affected by coating, a luciferase-expressing EnAd (EnAd(luc)) was coated as before and luciferase expression determined in HT-29 (epithelial colorectal adenocarinoma) cells. EnAd has previously been shown to display high oncolytic potency against this cell line with a 2-fold increase compared to Ad5(*44*) and it was therefore selected as an optimal model to assess its biological activity. Prior to these studies, cell metabolic activity was determined using an MTS assay 24 h. after exposure to the polymers alone (Figure S4). As no significant toxicity was found for these polymers at the concentration used and there was relatively little free polymer in a model reaction (Figure S3d), all the experiments were performed with virus-polymer conjugates without extensive purification from unreacted polymer.

Cells were treated with polymer-coated EnAd(luc) and an uncoated control and the luciferase expression was measured 24 h. post infection (Figure 5a). Transduction efficiency was markedly reduced for coated EnAd(luc) with up to 4-orders of magnitude reduction in luciferase expression compared to the uncoated control. There is no clear correlation between the shielding from neutralizing antibodies and the transduction efficiency, with virus coated with **P8**, which displayed high shielding efficiency at 1 mg/mL coating concentration, having one of the highest luciferase levels. Polymers with the higher level of diazonium modification, which showed more consistent and efficient coating, all reduced luciferase expression to the same level.

As *in vitro* results do not necessarily translate *in vivo*, **EnAd(luc)-P4** to **P9** were screened on naïve Balb/C mice to test gene transduction *in vivo* in the presence or absence of neutralizing serum (Figure 5b–d). Groups of three mice were injected intramuscularly with 1×10^9 vp/mouse. Luciferase expression was imaged using an IVIS imaging system and quantification performed at the site of injection, (Figure 5d, red circle).

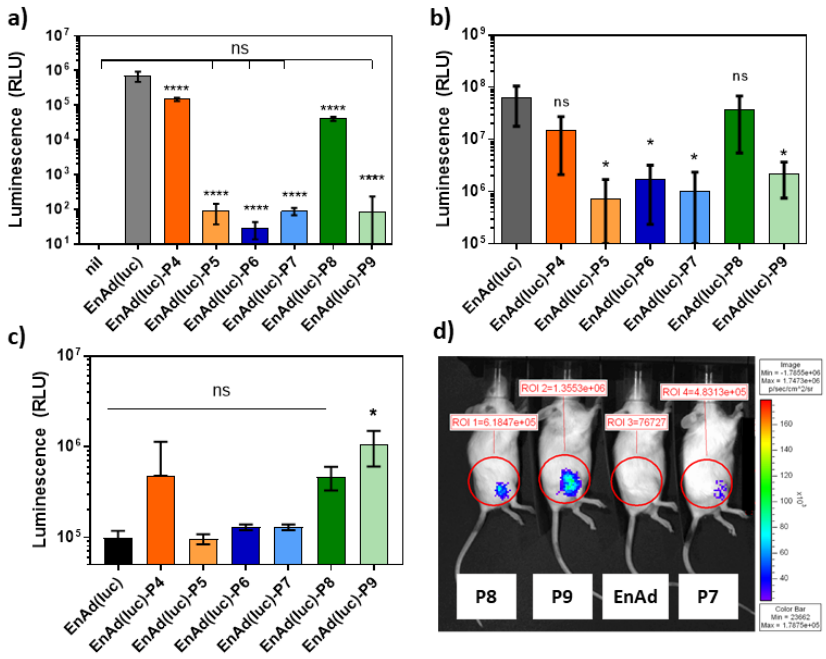

Figure 5. Transduction efficiency *in vitro* (a) and *in vivo* (b–d) of EnAd(luc) at 1 mg/mL polymer coating. a) Luciferase expression of HT-29 cells infected with 500 vp/cell of EnAd(luc) or polymer-coated EnAd(luc), measured 24 hours post infection. b, c and d) *In vivo* luciferase expression after intramuscular injection in Balb/C mice of 1×10^9 virus samples in PBS (b) and in neutralizing murine serum (c, d), measured at 24 hours post-injection using an IVIS imaging system. (Means of triplicate values and standard deviation, one-way ANOVA statistical analysis; graph a: $p < 0.0001$ vs EnAd(luc), ns vs uninfected cells (nil))(n=3),graph b; p=0.0255, graph c: p=0.0392.

When polymer-coated viruses were administered using phosphate-buffered saline (PBS) as the vehicle (Figure 5b), the luciferase expression was reduced in comparison to the uncoated virus in a similar manner to that seen *in vitro* albeit to a lesser extent. When neutralizing serum was used as a vehicle (Figure 5c and d), luciferase expression of the uncoated virus was reduced approximately 1000-fold compared to administration in PBS, demonstrating the high susceptibility of EnAd to neutralisation. Under these conditions, all formulations except **EnAd(luc)-P9** showed a reduction in transfection compared to administration in PBS.

EnAd(luc)-P9 maintained a significant level of luciferase expression, while expression levels similar to that of the uncoated control were observed for formulations **EnAd(luc)-P5** to **EnAd(luc)-P7. EnAd(luc)-P4** and **EnAd(luc)-P8**, which showed poor shielding in the ELISA, maintained more expression than the uncoated control but not to a significant level. These results indicate that polymeric features play an important role in imparting protection against

neutralising antibodies *in vivo*, with both longer polymer chain length and higher analine content being required to ensure sufficient protection.

Polymer coating delays EnAd cellular uptake and transgene expression

EnAd(luc)-P9 was selected for further investigations in order to obtain a better understanding of the intracellular mechanisms involved in the loss of viral activity after polymer coating. To allow separation of the effects of polymer coating on cell uptake and later downstream processes such as virus unpacking and trafficking, a "retargeted" virus was also produced. Poly(lysine) sequences of 6–10 residues are known to interact with cellular membranes via electrostatic interactions of the positively charged pendant amino groups and the negatively charged phospholipids and increase cell uptake.(*45*) Therefore, **P9** was functionalized with 1 mol% of oligolysine consisting of 7 amino acids (K_7) (Figure S5) which was then used to coat EnAd.

Uptake of **EnAd(luc)**, **EnAd(luc)-P9** and retargeted virus, **EnAd(luc)-P9-K$_7$**, viruses was quantified by qPCR. Cells were washed three times with PBS adjusted to pH 3 in order to detach any membrane-associated virus that could contribute to false positive results. The different uptake profiles of the three formulations are shown in Figure 6 where the coated virus, **EnAd(luc)-P9**, demonstrated a reduction in uptake compared to both **EnAd(luc)** and **EnAd(luc)-P9-K$_7$**.

Re-targeting not only restored uptake compared to **EnAd(luc)-P9** but was able to markedly improve it, most likely due to an increased interaction with the cell membrane that facilitated uptake through endocytic pathways other than receptor-mediated.(*45*) However, these results indicate that, although cellular uptake was involved in loss of transduction observed, this may not have been the only factor involved as the level of uptake was still high.

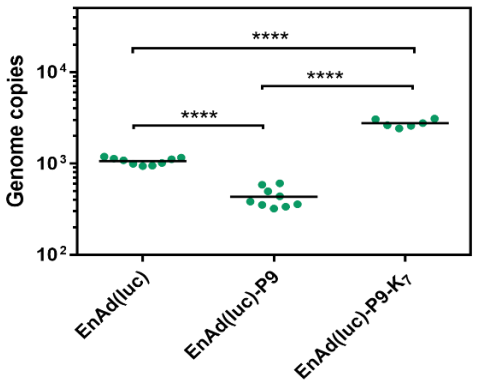

Figure 6. Viral uptake 1.5 hours post-infection. Viral genome copies were quantified by qPCR after three acid washes (PBS pH 3) to detach any membrane associated virus from the cells. Samples were prepared and analyzed in triplicate. Statistical analysis performed by one-way ANOVA, **** $p < 0.0001$.

Later time points were investigated to determine if the polymer coating was causing a delay in the unpackaging, a reduction of viral infectivity or a permanent inhibition due to hampered intracellular trafficking. HT-29 cells were infected for 1.5 h., washed with acidic PBS as described for the uptake studies, and incubated for 24, 48 and 72 h. Cells were then lysed and viral genome copies (qPCR) and transgene expression (luciferase assay) determined (Figure 7a and b). **EnAd(luc)** was able to replicate within the one day post infection, which corresponded to a high transgene expression (10^3 increase). Conversely, no significant replication was determined up to 3 days post-infection with **EnAd(luc)-P9** and **EnAd(luc)-P9-K7**. However, during the same time-course a steady increase of transgene expression became evident, with a faster expression mediated by **EnAd(luc)-P9-K7**. Luciferase expression is controlled by the immediate-early CMV promoter and requires partially disassembled virus escaping the endosome and reaching the cytoplasm.(*46*) These results indicate that the polymer-coating induces endosomal acculmation, or a delay in the unpackaging of the viral capsid, rather than a permanent inhibition. Accumulation in localised organelles at an early stage of infection was further confirmed by confocal fluorescence microscopy imaging (Figure S6).

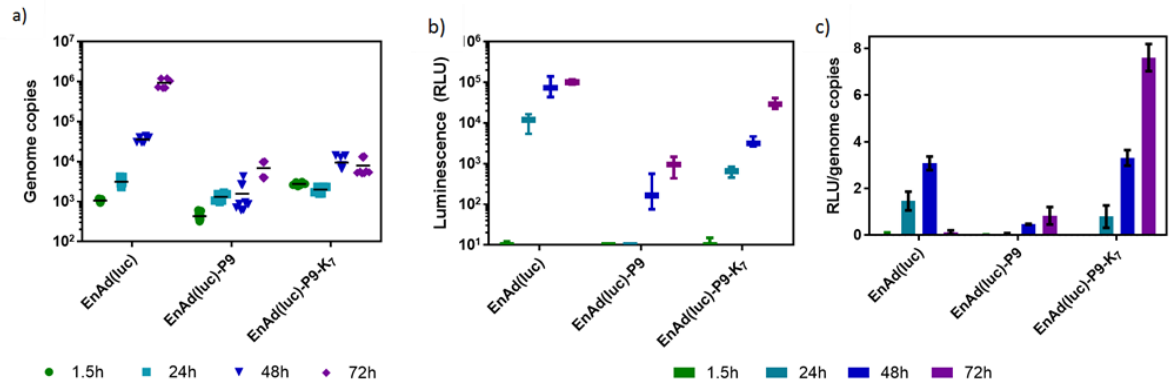

Figure 7. Viral disassembly and replication. Cells were infected with 500 vp/cell for 1.5 hours, washed three times with PBS pH 3 and, subsequently incubated at 37 °C, 5% CO2. Cells were lysed with 1x reporter lysis buffer at 1.5, 24, 48 and 72 h. post-infection. 25 µL of lysate was used to quantify viral genome copies by qPCR (a) and 25 µL to quantify transgene expression by luciferase reporter assay (b). C) "Specific transduction efficiency" calculated as RLU/genome copies ratio.

The "specific transduction efficiency", defined as the ratio of transgene expression per genome copies of internalised virus, seems to corroborate this hypothesis (Figure 7c). For **EnAd**, this increased in time until 72 h, when a drop was observed due to cell death. **EnAd(luc)-P9** showed a small increase in transduction efficiency in the same time-frame. Up to 48 h., **EnAd(luc)-P9-K$_7$** transduction efficiency was comparable to that of unmodified EnAd(Luc). However, a spike in luciferase activity was observed at 72 hours which may have arisen through different mechanisms such as the increased uptake of **EnAd-P9-K$_7$** and the possibility of K$_7$ aiding endosomal escape through membrane disruption by the charged alkyl amines.(*47*)

To investigate the effect of polymer-coating on replication, cell monolayers were infected with EnAd engineered to express green fluorescent protein (GFP) after replication has started (endogenous promoter SA, **EnAd(SA)**). **EnAd(SA)** was coated as before. The ability of **EnAd(SA)** to produce GFP positive cells allowed for visual observation of replication by fluorescence microscopy. Cells were infected with **EnAd(SA)**, **EnAd(SA)-P9** and **EnAd(SA)-P9-K$_7$** and imaged for up to 5 days post infection (Figure 8a).

For **EnAd(SA)**, GFP expression was detectable at 1 day post infection and achieved the highest levels at day 2; limited fluorescence was detected at day 3 due to significant cell death.

EnAd(SA)-P9 and **EnAd(SA)-P9-K$_7$** did not induce any significant fluorescence until 5 days post infection. Quantification of green fluorescence in the samples was performed by flow cytometry (Figure 8b). For **EnAd**, 60% of cells were GFP positive after two days. As observed by fluorescent microscopy, both the polymer-coated formulations, **EnAd(SA)-P9** and **EnAd(SA)-P9-K$_7$**, showed a slow onset of fluorescence which markedly increased at 5 days post infection at which point 80% of cells treated **EnAd(SA)-P9-K$_7$** were GFP positive. This enchancement of transgene expression is attributed to enhanced cell uptake provided by the K_7 targeting.

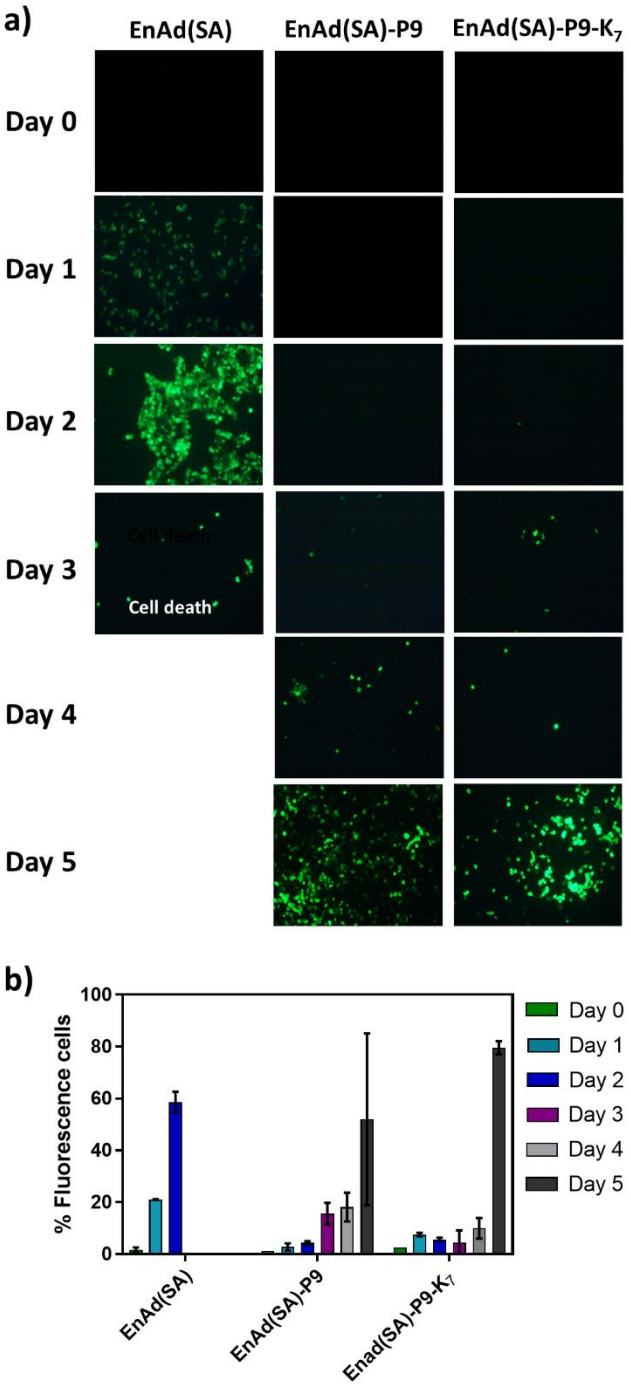

Figure 8. Green fluorescence micrographs (a) and percentage of fluorescent cellls (b) for HT-29 cells infected with EnAd(SA) GFP. Cells were infected with 100 vp/cell of EnAd(SA)-GFP, EnAd(SA)-P9, EnAd(SA)-P9-K_7. Images were recorded every 24 h. for 5 days using a widefield inverted microscope equipped with a green fluorescence filter. After imaging, cells were fixed for quantification using flow cytometry. Cells were detached from the well and fixed in 4 % PFA for 10 minutes at 4 C. After centrifugation, the pellet was resuspended in PBS and the percentage of GFP positive cells were quantified by flow cytometry.

These data together confirmed that the ability of **EnAd(SA)-P9** to replicate is not permanently hampered. The delayed onset of expression is in agreement with the delay in unpackaging, and suggestive that only a small number of viruses participated in the infection at this stage.

Consideration of the biological mechanisms underlying viral activity provide some explanations for the transfection and replication data observed. In EnAd(luc) is regulated under a cytomegalovirus (CMV) promoter which, when inserted in exogenous genetic materials, is constitutively active and allows luciferase to be expressed even when replication does not occur. In naïve mice, EnAd(luc) is replication-incompetent and luciferase expression thus reflects only the ability of the virus to enter cells and unpackage intracellularly. It is also important to recognise that the receptor used by EnAd, and in general by adenoviruses of species B, CD46, is not expressed in rodent cells.(*48*) For this reason, rodents are not ideal *in vivo* models when employed for testing with adenoviruses that enter cells through interactions with this receptor. However, in this study, the use of a rodent *in vivo* model was designed to serve as a 'background assay' to detect any uptake which might occur through the plethora of endocytic pathways. In particular, adenoviruses have been shown to induce cellular activation of macropinocytosis as a means to enter host cells, as reported by Amstutz *et al*. and Kalin *et al.* (*49*),[(50),(51)] for macropinocytic uptake of Ad3 and Ad35 in epithelial cells, respectively. These viruses also use CD46 as a receptor for epithelial cellular uptake, and thus can be considered to be analogous to EnAd in their cell internalisation properties. Both transgene expression and virus internalization assays in this study supported the hypothesis that different mechanisms, other than CD46 clathrin-dependent endocytosis, are involved in the internalization of EnAd. In addition, luciferase expression *in vivo* following polymer-coated EnAd administration was partly restored compared to that observed in the *in vitro* experiments. Interestingly, the effect of the different polymers resembled the trend observed for the *in vitro* screening and ELISA previously described. These data suggested that ligand-receptor

interactions play a pivotal role in ablating the activity of polymer-coated viruses *in vitro* but are not essential when the latter are administered *in vivo*. Polymers with higher diazonium content (**EnAd-P5**, **EnAd-P7** and **EnAd-P9**) and **EnAd-P6** could only partially restore transduction *in vivo*, with **EnAd-P9** recovering higher levels of luciferase expression compared to the other formulations. In a similar fashion, polydiazoniums of higher M_n (**EnAd-P8** and **EnAd-P9)** imparted enhanced protection against neutralizing mouse serum as compared to uncoated EnAd (Figure 5c and d). It is important to notice that although similar capsid-shielding and *in vitro* activity profiles were observed for **EnAd-P5, EnAd-P7** and **EnAd-P9** formulations**,** lower luciferase expression was induced by **EnAd-P5** and **EnAd-P7.** Taken together, these data allowed an insight into a structure-activity relationship of the investigated polymers which suggest that for the same content of reactive side-chain functionality, an increase in polymer size is favourable for both shielding and de-targeting purposes. It could be hypothesized that polymer coating interferes at the intracellular level, altering or limiting its natural trafficking. Successful infection by a virus relies on the delivery of viral genetic material to the host cell nuclei. A polymer that is too tightly bound to the viral surface could disrupt the tertiary structure of capsid proteins or sterically prevent capsid disassembly or endosomal escape, thus reducing the overall progress of the infection. When considering **EnAd-P5** and **EnAd-P9** (chain lengths 85 and 240, respectively) it might be expected that **EnAd-P9** would produce lower transgene expression *in vivo* compared to **EnAd-P5** due to the larger volume of the polymer. The result obtained could be attributed to the fact that a shorter polymer chain (polyHPMA **P1**, M_n ~ 12 kDa) can facilitate diazonium coupling by an increased exposure of the active groups compared to a more coiled and sterically hindered conformation of a longer polymer chain (pHPMA **P3**, M_n ~ 35 kDa). This would result in fewer azobenzene bonds being formed on **EnAd-P9** and a looser polymer coating, which is in agreement with the DLS results, through which prevention of antibody recognition would be mediated by steric

hindrance of this flexible and coiled structure as well as chemical blocking recognition sites. Consequently, **EnAd-P9** might allow increased viral disassembly compared to **EnAd-P5** or **EnAd7** as this looser coating will be more flexible. In contrast, if the polymer chains were tightly bound to the virus surface, capsid disassembly would be hindered. Since the DLS data demonstrated a marked increase in hydrodynamic volume of virus formulations as the polymer M_n increased, it is therefore likely that the longer polymers (**EnAd-P6** and **EnAd-P9**) bound in a more open structure to the virus surface. In turn, this higher entropy structure enhanced the steric shielding against large antibodies but did not completely prevent viral replication processes which arose through disassembly of smaller components at the viral capsid.

Conclusions

In this study, a novel set of functional polyHPMA-based materials bearing multiple diazonium salts was readily generated by simple and well-established coupling techniques via post-polymerization modifications. The broadened reactivity spectrum of diazonium salts towards various amino acids enabled optimized shielding of EnAd adenoviral capsid against neutralising antibody at polymer concentrations of 1 mg/mL, 10–20 fold lower than that reported in literature, as demonstrated *in vitro* and *in vivo*. Polymer chain length were found to be a key factor in both virus shielding and modulation of activity. Importantly, irreversible polymer conjugation with larger polymers did not result in permanent inactivation, as highlighted by time-course transgene expression and viral genome quantification, but likely a delayed unpackaging caused by impaired cellular trafficking. These data suggest that by further tailoring the polymer macromolecular features, it may be possible to tune key pharmaceutical properties of polymer-virus conjugates, such as circulation time, resistance to neutralising antibodies, internalisation and intracellular trafficking at target cells and to preserve viral activity.

Materials and Methods

Materials

1-amino-2-propanol (>99%), methacryloyl chloride (97%), (4-cyanopentanoic acid)-4-dithiobenzoate (CPADB), 4,4'-azobis(4-cyanovaleric acid) (V-501, >90%), azobis(isobutyronitrile) (AIBN, 98%), Fmoc-lysine(Boc), EDC (1-ethyl-3-(3-dimethylaminopropyl) carbodiimide), DMAP (4-dimethylamino pyridine), trifluoroacetic acid (TFA, 99%), sulfamic acid and triethylamine (TEA, >98%), Tris- Ethylenediaminetetraacetic acid (Tris-EDTA) were purchased from Sigma-Aldrich (Poole, UK). Sodium nitrite was purchased from Fluka. Di-*tert*-butyl-dicarbonate (97+%) were purchased from Alfa Aesar. Piperidine (>99%), anhydrous (<50 ppm water) N,N-dimethylacetamide (DMAc) and anhydrous (<50 ppm water) dimethylsulfoxide (DMSO) were purchased from Acros Organics (Geel, Belguim). 2-(7-Aza-1H-benzotriazole-1-yl)-1,1,3,3-tetra-methyluronium hexafluorophosphate (HATU, 98%) was purchased from Fluorochem Ltd (Hadfield, UK). H-NovaSyn®TGT resin was purchased from Novabiochem. High glucose Dulbecco's modified Eagle's Medium (DMEM) with L-glutamine, Dulbecco's phosphate buffer saline (DPBS), Hank's balanced salt solution (HBSS), fetal bovine serum (FBS) were purchased from Fisher scientific UK as well as all other chemicals and solvents (analytical or HPLC grade). AIBN was recrystallized from MeOH and methacryloyl chloride was distilled under Ar flow before use, all other chemicals were used as received unless otherwise stated. EnAd adenoviruses were supplied by PsiOxus Therapeutics: EnAd, EnAd(luc) (expressing firefly luciferase under CMV promoter), EnAd(SA) GFP (expressing green fluorescent protein under control of splicing acceptor).

Analytical Methods

Nuclear magnetic resonance (NMR) spectra were recorded on a Bruker Avance III 400 MHz spectrometer. All chemical shifts (δ) are reported in ppm relative to tetramethylsilane or

referenced to the chemical shifts of residual solvent resonances. Multiplicities are described with the following abbreviations: s = singlet, br = broad, d = doublet, t = triplet, m = multiplet. Mass spectrometry was carried out using a Micromass LCT ToF with electrospray ionization and OpenLynx software. Samples were prepared in 1:1 MeCN/water containing 0.1% v/v formic acid. Size exclusion chromatography (SEC) was performed on a Polymer Laboratories GPC 50 system equipped with a refractive index detector. Separations were achieved with a pair of PLgel Mixed-D (5 μm bead, 7.8 × 300 mm) columns with a matching guard (7.8 × 50 mm) and DMF containing 0.1% LiBr as eluent at a flow rate of 1 mL min^{-1}. Calibration was performed using narrow PMMA standards (Polymer Labs) in the molecular weight range 1-1200 kDa. Molecular weights and dispersity values were calculated using Cirrus GPC 3.0. Aqueous SEC was performed on Shimadzu Prominence UPLC system fitted with a DGU-20A5 degasser, LC-20AD low pressure gradient pump, CBM-20A LITE system controller, SIL-20A autosampler and an SPD-M20A diode array detector. Separations were performed on a PL Aquagel-OH 30 column (7.5 × 300 mm) with a mixture of 3:7 MeOH:PBS at a flow rate of 1.0 mL min^{-1} as the mobile phase.

Synthesis of *N*-(2-hydroxypropyl)methacrylamide (HPMA)

HPMA was prepared as previously described.(*52, 53*) Briefly, 1-amino-2-propanol (30 g, 0.40 mol) was dissolved in CH_2Cl_2 (800 mL) followed by the addition of solid $NaHCO_3$ (36 g, 0.44 mol). Freshly distilled methacryloyl chloride (40 g, 0.38 mol) was dissolved in CH_2Cl_2 (60 mL) and added to the suspension dropwise over the course of 1 h, at 0 °C. The reaction was allowed to proceed for 3 h. at room temperature. The suspension was filtered and the solvent removed under reduced pressure. The crude residue was recrystallized from acetone twice and the crystals dried under vacuum (42 g, 0.29 mol, 73%). ^{1}H NMR (400 MHz, $CDCl_3$): δ = 6.48 (br, 1H, N*H*), 5.73–5.69 (m, 1H, vinyl *Z* to Me-C=C), 5.37–5.30 (m, 1H, vinyl *E* to Me-C=C), 4.00–3.85 (m, 1H, C*H*OH), 3.53–3.43 (m, 1H, CH_aN), 3.28–2.95 (m, 2H, CH_bN + O*H*), 1.95

(s, 3H, C=C-C*H*3), 1.18 (dd, *J* = 6.3, 1.9 Hz, 3H, C*H*$_3$). ^{13}C NMR (100 MHz, CDCl3): δ = 169.55 (1C, C=O), 139.62 (1C, *C*=CH$_2$), 120.13 (1C, C=*C*H$_2$), 67.03 (1C, CHOH), 47.19 (1C, CH$_2$), 20.89 (1C, CH*C*H$_3$), 18.66 (1C, C*C*H$_3$). FT-IR: ν (cm^{-1}) = 3337, 2973, 1655, 1614, 1541. ESI-TOF-MS: m/z found 144.1011, [M+H]$^+$ requires 144.0980.

Synthesis of polyHPMA homopolymers

PolyHPMA homopolymers were synthesised by RAFT polymerization of HPMA following a known standard protocol.(*39*) Briefly, for the synthesis of pHPMA P1: HPMA (4.0 g, 28 mmol) was dissolved in acetate buffer (40 mL, pH 5.2, 1.0 M) along with CPADB (79 mg, 0.28 mmol) and V-501 (26 mg, 0.092 mmol). The solution was bubbled with nitrogen for 40 min before heating to 70 °C. Aliquots were taken periodically to monitor monomer conversion by ^{1}H NMR spectroscopy. Once a conversion of 70–85% was reached, the polymerisation was stopped by cooling the solution in an ice bath and exposing it to air. Polymers were subsequently purified by dialysis against water acidified with HCl (pH 3−4) using a 3.5 kDa MWCO membrane for 24 h and isolated by lyophilization. ^{1}H NMR (400 MHz, DMSO-d6): δ = 7.16 (broad s, 1H, CONH), 4.75 (broad s, 1H, CHO*H*), 3.76 (broad s, 1H, C*H*OH), 3.02 (broad s, 2H, CH$_2$), 1.74−1.00 (broad m, 8H, CH$_2$ and CH$_3$ of backbone and CHC*H$_3$*).

Chain Transfer Agent (CTA) end-group removal

Removal of the end group was performed according to the procedure described by Perrier et al.(*41*) A 30-fold molar excess of AIBN with respect to the chain transfer agent was employed. polyHPMA and AIBN were dissolved in dry DMSO and the solutions were bubbled with nitrogen for 35 min then heated to 80 °C for 3 h under continuous stirring. The resulting solutions were dialyzed against water for 24 h and subsequently lyophilized. The final thiol concentration was calculated using a standard Ellman's assay.(*54*) ^{1}H NMR (400 MHz, DMSO-d$_6$): δ = 7.16 (broad s, 1H, CONH), 4.75 (broad s, 1H, CHO*H*), 3.76 (broad s, 1H,

C*H*OH), 3.02 (broad s, 2H, CH_2), 1.74−1.00 (broad m, 8H, CH_2 and CH_3 of backbone and $CHCH_3$).

Synthesis of *N*-*t*-butoxycarbonyl-4-aminobenzoic acid

N-*t*-butoxycarbonyl-4-aminobenzoic acid was synthesized according to the protocol reported by Jones *et al.*(*42*) In a round bottomed flask, 4-aminobenzoic acid (2.5 g, 18 mmol) was dissolved in a mixture of 1,4-dioxane (35 mL) and water (20 mL). Triethylamine (5.0 mL, 37 mmol) was added to the solution and left under stirring for 10 minutes before addition of solid di-tert-butyl dicarbonate (8.0 g, 37 mmol). The reaction was allowed to proceed for 24 h. at room temperature. The solvent was removed under vacuum, then HCl_{aq} (3 M, 35 mL) was added to the residue to obtain a white precipitate that was recovered by filtration and freeze dried. The product was crystallized from hot methanol to yield *N*-*t*-butoxycarbonyl-4-aminobenzoic acid as a white solid (3.9 g, 91%). M.p. found 197-199 °C, reported 192-194 °C.(*55*) ^{1}H NMR (400 MHz, DMSO-d6): δ = 9.73 (s, 1H, CONH), 7.83 (d, 2H, J = 8.9 Hz, CH_{arom}), 7.55 (d, 2H, J = 8.9 Hz, CH_{arom}), 1.47 (s, 9H, 3 CCH_3). ^{13}C NMR (100 MHz, DMSO-d_6) δ (ppm) 167.1 (1C, COOH), 152.6 (1C, CONH), 143.8 (1C, *C*COOH), 130.4 (2C, CH), 124.0 (1C, CHNH), 117.2 (2C, CH), 79.7 (1C, $C(CH_3)_3$, 28.1 (3C, 3 CH_3). ESI-TOF-MS: m/z found 237.1529, $[M+H]^+$ requires 237.1001.

General procedure for the synthesis of Poly[HPMA]-r-[N-(2-hydroxypropyl)methacrylamide–4-(tert-butoxycarbonylamino)benzoate poly(HPMA-r-Boc-PABA)

Synthesis of HPMA-*r*-Boc-PABA **P9**: *N*-*t*-butoxycarbonyl-4-aminobenzoic acid (268 mg, 1.13 mmol) was dissolved in dry DMSO (5 mL). DMAP (276 mg, 2.22 mmol) and EDC (433 mg, 2.22 mmol) were subsequently added and allowed to dissolve under stirring for 10 min, after which polyHPMA (540 mg, 3.77 mmol) was added. The reaction was left to proceed for 36 h.

at room temperature; conversion was monitored by ^{1}H NMR spectroscopy. The crude product was first precipitated from Et_2O twice and, subsequently, purified by dialysis against water, using a 3.5 kDa cut-off, for 2 days and freeze dried. ^{1}H NMR (400 MHz, DMSO-d6): δ= 9.75 (br s, $CONH_{Boc}$), 7.87 (br s, CH_{arom}), 7.59 (br s, CH_{arom}), 7.13 (br s, $CONH_{HPMA}$), 4.96 (br s, 1H, CHOC(O)), 4.71 (br s, 1H, CHO*H*), 3.68 (br s, 1H, C*H*OH), 2.91 (br s, 2H, CH_2CH), 2.02-0.26 (br m, 17 H, CH_2CCH_3 $_{backbone}$, CHCH_3 and 3 $CH_{3\ Boc}$).

General procedure for the synthesis of poly[HPMA]-*r*-[N-(2-hydroxypropyl) methacrylamide–4-amino benzoate] poly(HPMA-*r*-PABA)

Poly(HPMA-*r*-Boc-PABA) **P9** (450 mg, 0.31 mmol of aniline) was dissolved in dry DMSO (7 mL) and to the resulting solution tetrabutylammonium fluoride (1.6 mL of 1M solution in THF, 1.6 mmol) was added. The reaction was allowed to proceed overnight at 80 °C under reflux. After cooling to room temperature, the final product was precipitated twice from Et_2O and, subsequently, purified by dialysis (3.5 kDa MWCO) against water for 1 day, and freeze-dried. ^{1}H NMR (400 MHz, DMSO-d6): δ= 7.66 (br s, 2CH_{arom}), 7.16 (br s, $CONH_{HPMA}$), 6.58 (br s, 2CH_{arom}), 5.92 (br s, 2H, $NH_{2aniline}$) 4.94 (br s, 1H, CHOCO), 4.73 (br s, 1H, CHO*H*), 3.68 (br s, 1H, C*H*OH), 2.91 (br s, 2H, CH_2CH), 2.15- 0.25 (br m, 17 H, CH_2CCH_3 $_{backbone}$, CHCH_3 and 3 CH_{3Boc}).

Synthesis of oligolysine-*N*-Boc (K_7)

A standard solid phase peptide synthesis procedure was used to synthesize oligolysine-N-Boc (K_7) peptide.(*56*) Seven *N*-Fmoc-Lys(Boc) were coupled in sequence to Fmoc-Lys(Boc) NovaSyn®TGT resin (750 mg, 0.13 mmol) using HATU as the coupling agent. The *N*-terminus was acetylated using 20% acetic anhydride in dry DMAc for 45 minutes. The peptide was cleaved from the resin using 0.1% TFA, 0.5% TIPS in dry DCM, the product dried under

reduced pressure and analyzed by HPLC and ESI-MS-ToF. ESI-TOF-MS: m/z found 1679.3453, 851.5477. $[M+Na]^+$ requires 1680.0421, $[M+2Na]^{2+}$ requires 851.5477.

Synthesis of re-targeting of polymer P9 with K_7 (P9-K_7)

Polymer **P9** (10 mg, 69.8 µmol of monomer units) was dissolved in DMSO-d6 (0.7 mL) along with K7 (2.3 mg, 1.4 µmol), EDC (27 mg, 0.140 mmol) and DMAP (4.3 mg, 34.9 µmol). The solution was allowed to react under stirring for 24 hours at room temperature. The product was purified by precipitation in mixture Et_2O: DCM 80:20 and twice in water before freeze drying the product. ^{1}H NMR (400 MHz, DMSO-d6): δ= 8.08-7.82 (s, $7NH_{Boc}$) 7.66 (br s, $2CH_{arom}$), 7.16 (br s, $CONH_{HPMA}$), 6.58 (br s,$2CH_{arom}$), 5.92 (br s, 2H, $NH_{2aniline}$) 4.94 (br s, 1H, CHOCO), 4.73 (br s, 1H, CHO*H*), 3.68 (br s, 1H, C*H*OH), 2.91 (br s, 2H, CH_2CH), 2.15- 0.25 (br m, 17 H, CH_2CCH_3 $_{backbone}$, CHCH_3 and 3 CH_{3Boc}).

General procedure for polymer coating of EnAd

Coating experiments were performed using a 10 mg/mL polymer stock solution. Typically, **P9** (3.0 mg, 5.0 µmol of aniline) was dissolved or suspended in HPLC grade water (150 µL) and 10% TFA in water (7.7 µL, 10.0 µmol) under stirring. The mixture was allowed to react for 45 min at room temperature, then cooled with an ice bath. 200 mg/mL $NaNO_2$ and of 150 mg/mL sulfamic acid stock solutions in water were placed in ice. Under vigorous stirring, ice cold $NaNO_2$ stock solution (3.5 µL) was added and incubated at 0 °C for 1 hour. Ice cold sulfamic acid stock solution (6.5 µL) was then added, and after 1 hour at 0 °C, the pH of the solution was adjusted to 7.4 with ice cold 500 mM HEPES pH 7.6 (132 µL). Polymer-coated virus stock solutions were prepared with a typical final titre of 5×10^{11} vp/mL in 50 mM HEPES buffer pH 7.4 at final polymer concentrations of 1 or 5 mg/mL. After addition of the polymer solution to the virus suspension, the conjugation reaction was allowed to proceed overnight at 4 °C. Formulations were aliquoted, flash frozen in liquid nitrogen and stored at -80°C.

Dynamic Light Scattering (DLS)

Particles size analyses were carried out at 25 °C using a Zetasizer Nano spectrometer (Malvern Instruments Ltd) equipped with a 633 nm laser at a fixed angle of 173°. Samples were suspended in HEPES buffer pH 7.4 10 mM.

Enzyme-Linked Immunosorbent Assay (ELISA)

A MaxiSorp™ NUNC ELISA plate was prepared by coating with 50 µL of 1:500 dilution of polyclonal rabbit anti-Ad capturing antibody (prepared by Morendum Scientific, Penicuik, UK) in 0.05 M pH 9.6 carbonate/ bicarbonate buffer overnight at 4°C. After incubation, the plate was washed four times with PBS, as for each incubation step of the procedure. Non-specific binding was prevented by incubation of 200 µL blocking solution, consisting of 5% BSA in PBS, for 1 hour. Next, 50 µL of 1×10^9 virus particles (vp)/mL virus formulations in blocking solution were incubated for 2 hours at room temperature. 50 µL of a 1:500 dilution of polyclonal mouse anti-Ad antibody (prepared in house by PsiOxus Therapeutics, Oxford, UK) was added to the wells. After 1 hour incubation at room temperature, 50 µL of 1: 300 dilution of goat anti-mouse HRP antibody (secondary antibody) in blocking solution were incubated for 1 hour. TMB-ELISA substrate was added to the plate ad incubated 20-30 min before stopping the reaction with 1N HCl. Absorbance was read at 450 nm.

Cell culturing conditions

For the *in vitro* studies, HT-29 human colorectal adenocarcinoma cells well cultured according to the procedures to the following procedures. Manufacturers or suppliers of reagents and equipments are stated where they are first mentioned. Laboratory plastic-ware was received by Fisher Scientific or Corning Inc. Cell culture media was high glucose Dulbecco's modified Eagle's Medium (DMEM) with L-glutamine and supplemented with 10% FBS ("growth media") or 2% FBS ("assay media").

Cell passage

HT-29 human epithelial colorectal adenocarcinoma cells were selected for this study (cell passage number 16 to 19). Cells were maintained at 37 °C, 5% CO_2 in a humidity-controlled incubator and all manipulations performed in a class II laminar flow cabinet. Cells were passaged when 80-90% confluency was reached. Specifically, cells were washed with PBS before treatment with Trypsin-EDTA (5 and 2 mL for T175 and T75 plasma treated flasks respectively) for 5-10 min at 37 °C, 5% CO_2. After detachment, cells were resuspended in fresh 10% FBS DMEM containing and split into a new flask containing fresh prewarmed growth media (dilution 1:10).

Cell plating

Cell suspensions were prepared as described above. After trypsinization, cells were pelleted and resuspended in DMEM containing 2% FBS (assay media). The concentration of live cells was determined using a hemocytometer to count cells and the concentration adjusted to the required one with fresh DMEM containing 2% FBS. Finally, cells were seeded into 96 well plate using a multi-channel pipette and allowed to attach overnight.

Luciferase Assay

Luciferase expression in HT-29 after transduction was measured using a Luciferase Reporter Assay System from Promega. Cells were seeded at a density of 30k cells/well on microplates in assay media. Infection was carried out with 500 vp/cell of EnAd(luc) formulations for 2 hours at 37 °C, 5% CO_2, followed by three PBS washes and incubation in fresh assay media. At the required time point, cells were washed with PBS before addition of 60 µL of lysis buffer. The plates were then frozen at -80°C overnight. After thawing the plates to room temperature cell lysates were resuspended and 25 µL transferred into half-area black well plates where 25 µL of luciferin was added. Luminescence readings were recorded for 10 s. as relative

luminescence units (RLU). The remaining cell lysates were used for genomic DNA extraction and quantification.

Quantitative PCR (qPCR)

As described above, cells seeded at 30k cells/well in assay media were infected with 500 vp/cell for 2 hours at 37 °C, 5% CO2 in microplates. After this time, cells were washed three times with PBS or pH 3 PBS and incubated for up to 72 h. in fresh assay media. At the desired time point, media was removed from the wells, 60 µL of 1× reporter lysis buffer were added and the plate frozen at -80°C overnight. A standard curve was obtained by addition of a known amount of virus to cells directly before addition of lysis buffer and the freezing process. Genomic DNA extraction was carried out using a GenElute Mammalian genomic DNA extraction kit as per the manufacturer's instructions. Briefly, samples were lysed with a lysis buffer and proteinase K at 70°C for 10 min before being loaded onto a DNA binding column. DNA was bound to the column and purified using ethanol containing buffers and finally eluted in a Tris-EDTA solution. A TaqMan® detection system was used to amplify and quantify genomic DNA from the samples. Probes labelled with 6-carboxyfluorescein (FAM) at 3' and tetramethylrhodamine (TAMRA) at 5'ends, forward and reverse primers specific for EnAd were added to qPCRBIO Probe Mix HI-ROX (PCR biosystem) and nuclease-free water added to a final volume of 12.5 µl per well, to obtain 125 nM of probe and 800 nM primers as final concentrations. 5 µl of samples were plated in PCR plates and sealed for analysis in a StepOnePlus™Real-Time PCR system (Applied Biosystem). The analysis was started at 50 °C for 2 min and 95°C for 10 min followed by 40 amplification cycles of 15 s. at 95°C and 90 s. at 60 °C, denaturation and annealing/extension steps respectively. Data were analysed using standard settings of StepOne™ Software.

Metabolic Activity Assay (MTS)

HT-29 cells were seeded into 96-well plate at a density of 25000 cell/well in 100 µL of assay media. Cells were treated with 1 mg/mL dilutions of polymer-coated EnAd in assay media and incubated for 2 hours at 37°C, 5% CO_2 before replacing the media with fresh one. After 24 hours incubation, cells were washed with PBS and 120 µL of a solution of MTS in phenol-red free assay media (1:6 dilution) added to the well. The plate was incubated for 30 min at 37°C, 5% CO_2 and the absorbance measured at 400 nm using Wallac 1420 Victor multi-label counter or BioTek™ Synergy HT multimodal microplate reader.

Live Confocal Microscopy

Uncoated EnAd was fluorescently labelled with a 20-fold molar excess per viral amine (approximately 1800 lysines per particle) of BODIPY-FL (Invitrogen) for 2 hours in 50 mM HEPES buffer at pH 7.4. Samples of polymer-coated EnAd were prepared according to the procedure described in previously, utilizing a 1 mg/mL final polymer concentration. Coating efficiency was tested by ELISA before conducting the experiments. 1×10^5 HT-29 cells were seeded on BD poly-L-Lysine glass bottomed 35 mm dishes and cultivated overnight in assay media. Cells were then washed with ice cold PBS, incubated in ice cold media (1.5 mL) before infection with 1×10^4 virus particles (uncoated EnAd or EnAd-P9- FL) for 1 hour over ice. After this time, cells were washed three times with ice cold PBS before addition of 1.5 mL of ice cold HBSS 20 mM HEPES buffer. The samples were stored on ice until they were placed in the incubation chamber for confocal imaging. Live cell imaging was performed on a LSM 710 (Carl Zeiss) confocal microscope using a 63× oil immersion objective and a CO_2-controlled incubator at 37 °C. Image analysis was performed using Zen Lite and ImageJ softwares. Images were digitized under constant exposure time, gain and offset.

Wide-field fluorescence microscopy

Samples of polymer-coated EnAd(SA) GFP were prepared according to the procedure described previously, utilizing a 1 mg/mL final polymer concentration. Coating efficiency was tested by ELISA before conducting the experiments. HT-29 cells were cultured in assay media at a density of 5×10^7 cells/well on 24 well plates overnight. Cells were infected with 100 vp/cell of polymer-coated EnAd(SA) for 2 hours, before washing three times with PBS. DMEM supplemented with 2% FBS was then added and cells incubated at 37 °C, 5% CO_2. Brightfield and fluorescence images were taken at defined time points using an inverted fluorescence microscope (Axiovert 25, Carl Zeiss) equipped with a 10× objective. Images were digitized under constant exposure time, gain and offset. After imaging the samples were collected for flow cytometry analysis.

Flow cytometry

After imaging, the samples were treated with cell dissociation buffer in PBS (Life Sciences) until complete cell detachment was obtained. Cells were then transferred into FACS tubes and pelleted by centrifugation at 300 g for 5 minutes. The pellet was then fixed using 4% paraformaldehyde for 15 minutes at 4 °C, re-pelleted and resuspended in PBS. Fluorescent cells were counted using FACSCaliber (Becton Dickinson) and analyzed using CellQuestPro and FlowJo software. The experiment was run in triplicate.

In vivo studies

All *in vivo* studies were conducted in accordance with institutional ethics procedures and UK Home Office authorisation (Animal Scientific Procedures Act 1986) under project license 30/2819. Female Balb/C mice were obtained from Charles River Laboratories at 4-6 weeks old. Mice were housed in a temperature- and humidity-controlled conditions (20-22 °C) in

individually ventilated cages at the John Radcliffe Hospital, Oxford. Mice were given free access to sterilised tap water and formulated diets, and exposed to 12 h. light-dark cycles.

In vivo luciferase expression in the absence and presence of neutralizing mice serum

Samples of the polymer-coated EnAd were prepared according to the procedure described above, utilizing a 1 mg/mL final polymer concentration. EnAd stock suspension was diluted in PBS or in anti-EnAd hyperimmune mice serum (prepared in-house by PsiOxus Therapeutics) to a concentration of 5×10^9 vp/mL. One intramuscular injection of 1×10^9 virus particles (20 µL) of each sample was performed in each flank of female naÏve Balb/C mice. Luciferase expression was measured at 24 hours post-injection using an IVIS imaging system.

Conflicts of interest

DC, SI and KF are current and former employees of PsiOxus Therapeutics. KF and LWS have commercial interests in PsiOxus Therapeutics. NF, GM, CA and SGS have received funding from PsiOxus Therapeutics.

Acknowledgements

This work was supported by the Engineering and Physical Sciences Research Council (Grants EP/H005625/1, EP/N03371X/1), the Royal Society (Wolfson Research Merit Award WM150086) and PsiOxus Therapeutics Ltd for funding this work. We also gratefully acknowledge Paul Cooling, Esme Ireson, Tom Booth and Christine Grainger-Boultby for expert technical assistance.

Supporting Information

This material is available free of charge via the Internet at http://pubs.acs.org. UV-Visible spectra before and after end group removal; NMR spectra of *N*-*t*-butoxycarbonyl-4-aminobenzoic acid; electrophoresis, DLS and GPC data for the model conjugation to BSA; cell metabolic activity assay after treatment with polymers, NMR spectra of P9-K_7; live confocal microscopy in HT-29 cells.

Data access statement

All raw data created during this research are openly available from the corresponding author (Cameron.alexander@nottingham.ac.uk) and at the University of Nottingham Research Data Management Repository (https://rdmc.nottingham.ac.uk/) and all analyzed data supporting this study are provided as supplementary information accompanying this paper.

References

(1) Wheelock, E. F., and Dingle, J. H. (1964) Observations on the repeated administration of viruses to a patient with acute leukemia. *New Engl. J. Med. 271*, 645-651.
(2) Asada, T. (1974) Treatment of human cancer with mumps virus. *Cancer 34*, 1907-1928.
(3) Peng, K. W., Hadac, E. M., Anderson, B. D., Myers, R., Harvey, M., Greiner, S. M., Soeffker, D., Federspiel, M. J., and Russell, S. J. (2006) Pharmacokinetics of oncolytic measles virotherapy: eventual equilibrium between virus and tumor in an ovarian cancer xenograft model. *Cancer Gene Ther. 13*, 732-8.
(4) Doyle, T. C., Burns, S. M., and Contag, C. H. (2004) In vivo bioluminescence imaging for integrated studies of infection. *Cell Microbiol. 6*, 303-17.
(5) McFadden, G., Mohamed, M. R., Rahman, M. M., and Bartee, E. (2009) Cytokine determinants of viral tropism. *Nat. Rev. Immunol. 9*, 645-655.
(6) Yu, W., and Fang, H. (2007) Clinical Trials with Oncolytic Adenovirus in China. *Curr. Cancer Drug Tar. 7*, 141-148.
(7) Jia, H., and Kling, J. (2006) China offers alternative gateway for experimental drugs. *Nat. Biotech. 24*, 117-118.
(8) Pol, J., Kroemer, G., and Galluzzi, L. (2016) First oncolytic virus approved for melanoma immunotherapy. *Oncoimmunology 5*, e1115641.
(9) Garcia-Aragoncillo, E., and Hernandez-Alcoceba, R. (2010) Design of virotherapy for effective tumor treatment. *Curr. Opin. Mol. Ther. 12*, 403-411.
(10) Corbo, C., Molinaro, R., Tabatabaei, M., Farokhzad, O. C., and Mahmoudi, M. (2017) Personalized protein corona on nanoparticles and its clinical implications. *Biomater. Sci. 5*, 378-387.

(11) Du, F.-S., Wang, Y., Zhang, R., and Li, Z.-C. (2010) Intelligent nucleic acid delivery systems based on stimuli-responsive polymers. *Soft Matter 6*, 835-848.
(12) Ruiz-Hernandez, E., Hess, M., Melen, G. J., Theek, B., Talelli, M., Shi, Y., Ozbakir, B., Teunissen, E. A., Ramirez, M., Moeckel, D., Kiessling, F., Storm, G., Scheeren, H. W., Hennink, W. E., Szalay, A. A., Stritzker, J., and Lammers, T. (2014) PEG-pHPMAm-based polymeric micelles loaded with doxorubicin-prodrugs in combination antitumor therapy with oncolytic vaccinia viruses. *Polym. Chem. 5*, 1674-1681.
(13) Li, J., Mao, H., Kawazoe, N., and Chen, G. (2017) Insight into the interactions between nanoparticles and cells. *Biomater. Sci. 5*, 173-189.
(14) Liao, W.-Y., Li, H.-J., Chang, M.-Y., Tang, A. C. L., Hoffman, A., and Hsieh, P. C. H. (2013) Comprehensive Characterizations of Nanoparticle Biodistribution Following Systemic Injection in Mice. *Nanoscale 5*, 11079-86.
(15) Zhou, J., and Chau, Y. (2016) Different oligoarginine modifications alter endocytic pathways and subcellular trafficking of polymeric nanoparticles. *Biomater. Sci. 4*, 1462-1472.
(16) Hovlid, M. L., Lau, J. L., Breitenkamp, K., Higginson, C. J., Laufer, B., Manchester, M., and Finn, M. G. (2014) Encapsidated Atom-Transfer Radical Polymerization in Q beta Virus-like Nanoparticles. *ACS Nano 8*, 8003-8014.
(17) Hovlid, M. L., Steinmetz, N. F., Laufer, B., Lau, J. L., Kuzelka, J., Wang, Q., Hyypia, T., Nemerow, G. R., Kessler, H., Manchester, M., and Finn, M. G. (2012) Guiding plant virus particles to integrin-displaying cells. *Nanoscale 4*, 3698-3705.
(18) Pokorski, J. K., Breitenkamp, K., Liepold, L. O., Qazi, S., and Finn, M. G. (2011) Functional Virus-Based Polymer-Protein Nanoparticles by Atom Transfer Radical Polymerization. *J. Am. Chem. Soc. 133*, 9242-9245.
(19) Fisher, K. D., Green, N. K., Hale, A., Subr, V., Ulbrich, K., and Seymour, L. W. (2007) Passive tumour targeting of polymer-coated adenovirus for cancer gene therapy. *J. Drug Target. 15*, 546-551.
(20) Lee, P. W., Isarov, S. A., Wallat, J. D., Molugu, S. K., Shukla, S., Sun, J. E. P., Zhang, J., Zheng, Y., Dougherty, M. L., Konkolewicz, D., Stewart, P. L., Steinmetz, N. F., Hore, M. J. A., and Pokorski, J. K. (2017) Polymer Structure and Conformation Alter the Antigenicity of Virus-like Particle-Polymer Conjugates. *J. Am. Chem. Soc. 139*, 3312-3315.
(21) Pokorski, J. K., and Steinmetz, N. F. (2011) The Art of Engineering Viral Nanoparticles. *Mol. Pharmaceutics 8*, 29-43.
(22) Carlisle, R., Choi, J., Bazan-Peregrino, M., Laga, R., Subr, V., Kostka, L., Ulbrich, K., Coussios, C. C., and Seymour, L. W. (2013) Enhanced tumor uptake and penetration of virotherapy using polymer stealthing and focused ultrasound. *J. Natl Cancer Inst. 105*, 1701-10.
(23) O'Riordan, C. R., Lachapelle, A., Delgado, C., Parkes, V., Wadsworth, S. C., Smith, A. E., and Francis, G. E. (1999) PEGylation of adenovirus with retention of infectivity and protection from neutralizing antibody in vitro and in vivo. *Hum. Gene Ther. 10*, 1349-58.
(24) Croyle, M. A., Yu, Q. C., and Wilson, J. M. (2000) Development of a rapid method for the PEGylation of adenoviruses with enhanced transduction and improved stability under harsh storage conditions. *Hum. Gene Ther. 11*, 1713-22.
(25) Manzenrieder, F., Luxenhofer, R., Retzlaff, M., Jordan, R., and Finn, M. G. (2011) Stabilization of Virus-like Particles with Poly(2-oxazoline)s. *Angew. Chem. Int. Ed. 50*, 2601-2605.
(26) Fisher, K. D., and Seymour, L. W. (2010) HPMA copolymers for masking and retargeting of therapeutic viruses. *Adv. Drug Deliver. Rev. 62*, 240-245.

(27) Fisher, K. D., Stallwood, Y., Green, N. K., Ulbrich, K., Mautner, V., and Seymour, L. W. (2001) Polymer-coated adenovirus permits efficient retargeting and evades neutralising antibodies. *Gene Ther. 8*, 341-8.
(28) Li, S., Chen, J., Xu, H., Long, J., Xie, X., and Zhang, Y. (2014) The Targeted Transduction of MMP-Overexpressing Tumor Cells by ACPP-HPMA Copolymer-Coated Adenovirus Conjugates. *PLoS ONE 9*, e100670.
(29) Fisher, K. D., Green, N. K., Hale, A., Subr, V., Ulbrich, K., and Seymour, L. W. (2007) Passive tumour targeting of polymer-coated adenovirus for cancer gene therapy. *J Drug Target 15*, 546-51.
(30) Lanciotti, J., Song, A., Doukas, J., Sosnowski, B., Pierce, G., Gregory, R., Wadsworth, S., and O'Riordan, C. (2003) Targeting Adenoviral Vectors Using Heterofunctional Polyethylene Glycol FGF2 Conjugates. *Mol. Ther. 8*, 99-107.
(31) Morrison, J., Briggs, S. S., Green, N., Fisher, K., Subr, V., Ulbrich, K., Kehoe, S., and Seymour, L. W. (2007) Virotherapy of Ovarian Cancer With Polymer-cloaked Adenovirus Retargeted to the Epidermal Growth Factor Receptor. *Mol. Ther. 16*, 244-251.
(32) Stevenson, M., Hale, A. B., Hale, S. J., Green, N. K., Black, G., Fisher, K. D., Ulbrich, K., Fabra, A., and Seymour, L. W. (2007) Incorporation of a laminin-derived peptide (SIKVAV) on polymer-modified adenovirus permits tumor-specific targeting via alpha6-integrins. *Cancer Gene Ther. 14*, 335-45.
(33) Subr, V., Kostka, L., Selby-Milic, T., Fisher, K., Ulbrich, K., Seymour, L. W., and Carlisle, R. C. (2009) Coating of adenovirus type 5 with polymers containing quaternary amines prevents binding to blood components. *J. Control. Release 135*, 152-158.
(34) Green, N. K., Herbert, C. W., Hale, S. J., Hale, A. B., Mautner, V., Harkins, R., Hermiston, T., Ulbrich, K., Fisher, K. D., and Seymour, L. W. (2004) Extended plasma circulation time and decreased toxicity of polymer-coated adenovirus. *Gene Ther. 11*, 1256-63.
(35) Rux, J. J., and Burnett, R. M. (2004) Adenovirus structure. *Hum. Gene Ther. 15*, 1167-76.
(36) Marino, N., Illingworth, S., Kodialbail, P., Patel, A., Calderon, H., Lear, R., Fisher, K. D., Champion, B. R., and Brown, A. C. N. (2017) Development of a versatile oncolytic virus platform for local intra-tumoural expression of therapeutic transgenes. *PLOS ONE 12*, e0177810.
(37) Garcia-Carbonero, R., Salazar, R., Duran, I., Osman-Garcia, I., Paz-Ares, L., Bozada, J. M., Boni, V., Blanc, C., Seymour, L., Beadle, J., Alvis, S., Champion, B., Calvo, E., and Fisher, K. (2017) Phase 1 study of intravenous administration of the chimeric adenovirus enadenotucirev in patients undergoing primary tumor resection. *J. Immunother. Cancer 5*, 71.
(38) Francini, N., Purdie, L., Alexander, C., Mantovani, G., and Spain, S. G. (2015) Multifunctional Poly N-(2-hydroxypropyl)methacrylamide Copolymers via Postpolymerization Modification and Sequential Thiol-Ene Chemistry. *Macromolecules 48*, 2857-2863.
(39) Scales, C. W., Vasilieva, Y. A., Convertine, A. J., Lowe, A. B., and McCormick, C. L. (2005) Direct, Controlled Synthesis of the Nonimmunogenic, Hydrophilic Polymer, Poly(N-(2-hydroxypropyl)methacrylamide) via RAFT in Aqueous Media†. *Biomacromolecules 6*, 1846-1850.
(40) Pissuwan, D., Boyer, C., Gunasekaran, K., Davis, T. P., and Bulmus, V. (2010) In Vitro Cytotoxicity of RAFT Polymers. *Biomacromolecules 11*, 412-420.

(41) Perrier, S., Takolpuckdee, P., and Mars, C. A. (2005) Reversible addition-fragmentation chain transfer polymerization: End group modification for functionalized polymers and chain transfer agent recovery. *Macromolecules 38*, 2033-2036.
(42) Jones, M. W., Mantovani, G., Blindauer, C. A., Ryan, S. M., Wang, X., Brayden, D. J., and Haddleton, D. M. (2012) Direct Peptide Bioconjugation/PEGylation at Tyrosine with Linear and Branched Polymeric Diazonium Salts. *J. Am. Chem. Soc. 134*, 7406-7413.
(43) Chen, X., Zhang, Y., Liu, B., Zhang, J., Wang, H., Zhang, W., Chen, Q., Pei, S., and Jiang, Z. (2008) Novel photoactive hyperbranched poly(aryl ether)s containing azobenzene chromophores for optical storage. *J. Mater. Chem. 18*, 5019-5026.
(44) Kuhn, I., Harden, P., Bauzon, M., Chartier, C., Nye, J., Thorne, S., Reid, T., Ni, S., Lieber, A., Fisher, K., Seymour, L., Rubanyi, G. M., Harkins, R. N., and Hermiston, T. W. (2008) Directed Evolution Generates a Novel Oncolytic Virus for the Treatment of Colon Cancer. *PLoS ONE 3*, e2409.
(45) Wang, C.-H. K., Chan, L. W., Johnson, R. N., Chu, D. S. H., Shi, J., Schellinger, J. G., Lieber, A., and Pun, S. H. (2011) The transduction of Coxsackie and Adenovirus Receptor-negative cells and protection against neutralizing antibodies by HPMA-co-oligolysine copolymer-coated adenovirus. *Biomaterials 32*, 9536-9545.
(46) Hermiston, T. W., Malone, C. L., and Stinski, M. F. (1990) Human cytomegalovirus immediate-early two protein region involved in negative regulation of the major immediate-early promoter. *J. Virol. 64*, 3532-3536.
(47) Hong, S., Leroueil, P. R., Janus, E. K., Peters, J. L., Kober, M.-M., Islam, M. T., Orr, B. G., Baker, J. R., and Banaszak Holl, M. M. (2006) Interaction of Polycationic Polymers with Supported Lipid Bilayers and Cells: Nanoscale Hole Formation and Enhanced Membrane Permeability. *Bioconjugate Chem. 17*, 728-734.
(48) Kemper, C., Leung, M., Stephensen, C. B., Pinkert, C. A., Liszewski, M. K., Cattaneo, R., and Atkinson, J. P. (2001) Membrane cofactor protein (MCP; CD46) expression in transgenic mice. *Clin. Exp. Immunol. 124*, 180-189.
(49) Meier, O., Boucke, K., Hammer, S. V., Keller, S., Stidwill, R. P., Hemmi, S., and Greber, U. F. (2002) Adenovirus triggers macropinocytosis and endosomal leakage together with its clathrin-mediated uptake. *J. Cell Biol. 158*, 1119-1131.
(50) Kälin, S., Amstutz, B., Gastaldelli, M., Wolfrum, N., Boucke, K., Havenga, M., DiGennaro, F., Liska, N., Hemmi, S., and Greber, U. F. (2010) Macropinocytotic Uptake and Infection of Human Epithelial Cells with Species B2 Adenovirus Type 35. *J. Virol. 84*, 5336-5350.
(51) Amstutz, B., Gastaldelli, M., Kälin, S., Imelli, N., Boucke, K., Wandeler, E., Mercer, J., Hemmi, S., and Greber, U. F. (2008) Subversion of CtBP1-controlled macropinocytosis by human adenovirus serotype 3. *EMBO J. 27*, 956-969.
(52) Ulbrich, K., Šubr, V., Strohalm, J., Plocová, D., Jelínková, M., and Říhová, B. (2000) Polymeric drugs based on conjugates of synthetic and natural macromolecules: I. Synthesis and physico-chemical characterisation. *J. Control. Release 64*, 63-79.
(53) Rowe, M. D., Chang, C.-C., Thamm, D. H., Kraft, S. L., Harmon, J. F., Vogt, A. P., Sumerlin, B. S., and Boyes, S. G. (2009) Tuning the Magnetic Resonance Imaging Properties of Positive Contrast Agent Nanoparticles by Surface Modification with RAFT Polymers. *Langmuir 25*, 9487-9499.
(54) Ellman, G. L., Courtney, K. D., Andres, V., and Featherstone, R. M. (1961) A new and rapid colorimetric determination of acetylcholinesterase activity. *Biochem. Pharmacol. 7*, 88-95.

(55) Reddington, S. C., Baldwin, A. J., Thompson, R., Brancale, A., Tippmann, E. M., and Jones, D. D. (2015) Directed evolution of GFP with non-natural amino acids identifies residues for augmenting and photoswitching fluorescence. *Chem. Sci. 6*, 1159-1166.
(56) Coin, I., Beyermann, M., and Bienert, M. (2007) Solid-phase peptide synthesis: from standard procedures to the synthesis of difficult sequences. *Nat. Protocols 2*, 3247-3256.

TOC Graphic